# The Influence of Temporal Discretization Regarding Lighthill's Source Terms of an Automotive Turbocharger Compressor

Clemens Freidhager[1], Stefan Schoder[2], Manfred Kaltenbacher[3,4]

[1] Technische Universität Wien, 1040 Wien, Österreich, Email: clemens.freidhager@tuwien.ac.at

[2] Technische Universität Wien, 1040 Wien, Österreich, Email: stefan.schoder@tuwien.ac.at

[3] Technische Universität Wien, 1040 Wien, Österreich, Email: manfred.kaltenbacher@tuwien.ac.at

[4] Technische Universität Graz, 8010 Graz, Österreich, Email: manfred.kaltenbacher@tugraz.at

## Introduction

Due to improvements regarding electric engine injection, the noise generated by a combustion engine has been significantly decreased over the last years. Consequently, a major remaining noise source of a car is the turbocharger. Therefore, a hybrid aeroacoustics method, considering Lighthill's analogy, is applied for investigating source term mechanism. Thereby, the influence of different time steps onto results of the Computational Fluid Dynamic (CFD) simulations, and of Lighthill's stress tensor are investigated. Therefore, all three parts of Lighthill's source term, (1) the Reynolds stress term, (2) the excess term, and the (3) viscous term will be analyzed in time and frequency domain.

## Lighthill's Analogy

For deriving Lighthill's analogy [1] a confined fluctuating fluid in a much larger region at rest is considered. The large region at rest is assumed to be an ideal linear acoustic medium with a pressure $p_0$, a density $\rho_0$, and speed of sound $c_0$. Then the equations governing density fluctuations, the general equations of mass and momentum conservation, in those two regions are compared, bringing up Lighthill's equation, an exact inhomogeneous wave equation

$$\left(\frac{1}{c_0^2}\frac{\partial^2}{\partial t^2} - \Delta\right)(c_0^2(\rho-\rho_0)) = \nabla\cdot\nabla\cdot[\boldsymbol{T}]\,, \qquad (1)$$

with $[\boldsymbol{T}]$ being Lighthill's stress tensor. Lighthill's equation is an exact reformulation, without simplifications, and describes all possible aerodynamic and aeroacoustic pressure production and propagation mechanisms. Lighthill's stress tensor $[\boldsymbol{T}]$, is also referred to as Lighthill's aeroacoustic source term, and couples the flow and acoustic field. It can be subdivided into three main parts, the Reynolds stresses (I), an excess term (also referred to as entropy term) (II), and a viscous term (III)

$$[\boldsymbol{T}] = \underbrace{\rho\boldsymbol{v}\otimes\boldsymbol{v}}_{\text{I}} + \underbrace{((p-p_0)-c_0^2(\rho-\rho_0))[\boldsymbol{I}]}_{\text{II}} - \underbrace{[\boldsymbol{\tau}]}_{\text{III}}\,. \qquad (2)$$

The Reynold stress term incorporates the convection of sound with the flow. For flows with low Mach number $Ma$ the principal generators of sound are the fluctuating Reynolds stresses, with a proportional error of order $\mathcal{O}(Ma^2)$ [2]. Consequently, for incompressible flows the excess and viscous term can be neglected [3, 4].

The excess term represents the excess of momentum transfer by the pressure over that in the ideal linear acoustic medium, which is produced by mean density variations in the source flow [5]. Pressure and density within a flow are related by the local speed of sound $c$ ($p = c^2\rho$) [4]. As a result, if the temperature $T$ in the spatially limited fluctuating fluid is not very different to the temperature $T_0$ in the large region at rest, $c \approx c_0$ will hold and the influence of the excess term will be small. The relation between temperature $T$ and density $\rho$ for gases comes from the definition of density

$$\rho = \frac{m}{V}\,, \qquad (3)$$

with $m$ as mass and $V$ as volume, and is described by Charles's law [6], stating that for $p = \text{const.}$

$$V \propto T\,, \qquad (4)$$

holds. Consequently, the excess term is responsible for thermoacoustic effects [2]. Furthermore, it can be stated that with the excess term, sound propagation with variable speed of sound and gradual dissipation by conduction is considered [1].

In the spatially limited fluctuating flow Reynolds number $Re$ is usually very high and therefore the viscous term is very small, and can be neglected. Furthermore, the dissipation of acoustic energy into heat due to viscosity and heat conduction is a very slow process requiring very large distances in order of atmospheric scales, to show a noteworthy influence on propagation [1].

## Computational Fluid Dynamics

A fundamental decision regarding transient CFD simulations is which time step is used. For CFD simulations of turbocharger compressors, a widely used method is to use a time step that corresponds to the time it takes the wheel to turn 1° [7, 8, 9]. Consequently, a dimensionless time is used to define the time step. To investigate the influence of this method onto global measurements, as well as onto local pressure fluctuations, and especially onto Lighthill's source terms, a compressible transient CFD simulation using StarCCM+ was established. Therefore, a Detached Eddy Simulation (DES) with an underlying $k-\omega$ Shear Stress Transport (SST) turbulence model was used. The simulation setup consists of about 3.5 million cells, with significant mesh refinements at the tip-gap

between wheel and housing, and close to blade surfaces. Furthermore, 10 prism layers are used for discretization of boundary layers. Compared to literature [8, 7] this is a comparatively coarse mesh. However, the CFD grid is restricted by the amount of data arising by investigating the field of source terms in the frequency domain. Furthermore, the all $y+$ wall treatment of StarCCM+ was applied for resolving boundary layers with varying $y+$ values. Additionally, to ensure non-reflective inlet and outlet boundaries, which is especially important for compressible flows, the inlet and outlet was extruded by 10 times the diameter with increasing cell ratio. As inlet boundary condition a mass flow inlet, and as outlet boundary condition a pressure outlet was applied. For the impeller region a rigid body rotation was used, and for temporal discretization a second order scheme was considered.

Furthermore, a point near the highest efficiency with $n = 120000$ 1/min was chosen as the operating point of the turbocharger compressor, because at such operation points no flow separation inside the impeller is expected. This brings two advantages. Firstly, less turbulent structures occur without flow separation, which means that the simulation results can be better interpreted. Secondly, using a comparatively coarse CFD mesh, results at $y+ > 1$ for some parts of the wheel surface. For $y+ > 1$ the all $y+$ wall treatment automatically applies wall functions, which are known to deliver poor results for flow conditions with separation from the wheel blade surfaces. As a result, an operation point without flow separation is more suitable for the coarse CFD mesh.

## Results

As a first task during the evaluation of the simulation results, it is checked if no backflow trough the impeller due to flow separation occurs. Therefore, the negative velocity component in axial direction is investigated (see Fig. 1). For validating the CFD simulation global measure-

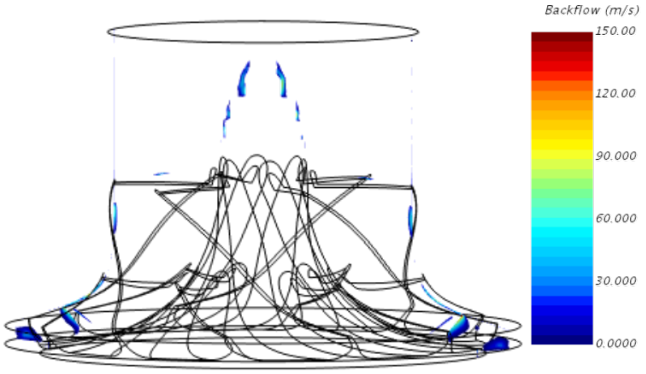


**Figure 1:** Backflow through the impeller.

ments, as the isentropic efficiency $\eta$, the pressure ratio $\Delta p$, and the mass flow $\dot{m}$, are investigated and compared with measurements of a hot gas test rig. Therefore, an average value over at least 5 turns is computed. In a next step, a relative error

$$E_{\square} = \frac{|\square_s - \square_m|}{\square_m} \cdot 100\%\,, \tag{5}$$

with $\square_m$ as measurements and $\square_s$ as results of the simulation, was computed bringing up the following relative errors (see Table. 1). For evaluating the simulation results of local pressure-time-signals ($p-t-$signal) of one certain evaluation point, a quantitative comparison is performed. Therefore, FFTs of 15 converged rotations of the $p-t-$signal of the evaluation point (see Fig. 2) were computed. This showed no major differences in the

| | Time step per turn | | |
|---|---|---|---|
| | 360 | 596 | 720 |
| $E_\eta$ in % | 0.39 | 0.48 | 0.23 |
| $E_{\Delta p}$ in % | 0.15 | 0.28 | 0.29 |
| $E_{\dot{m}}$ in % | 0.55 | 0.01 | 0.87 |

**Table 1:** Relative errors $E_{\square}$ of global quantities, of simulation results and measurements of a hot gas rig.

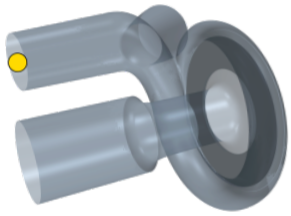

**Figure 2:** Evaluation point used for validating CFD simulation locally.

spectra of the $p-t-$signal. However, differences with small amplitudes, which are probably connected to turbulent structures, occurred (see Fig. 3) The increase of

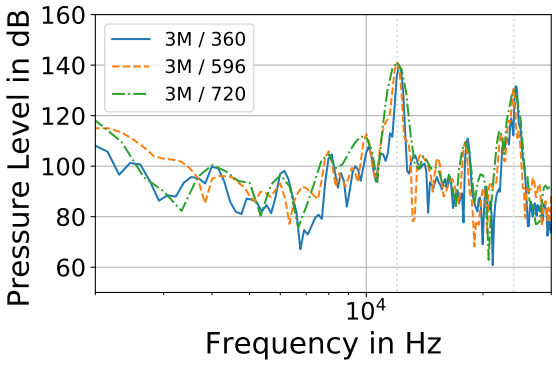


**Figure 3:** Spectra of simulations with three different time steps of a $p-t-$signal of a discrete evaluation point, with the BPF $f_{\text{Blade}}$ depicted as grey, dotted line.

the spectra at low frequency range can be connected with the used kaiser window function applied, to reduce leakage.

## Source Terms

The flow inside of the turbocharger compressor has a very high Mach number $Ma$ and therefore is highly compressible. Consequently, it is estimated that the excess term can not be neglected. For investigation purposes Lighthill's source terms of two revolutions were post-processed. The source terms were weighted with the cell volume, and a field FFT was computed. Finally, the absolute value of the FFT amplitudes were averaged over all cells. It could be shown, that the dominant Lighthill source term is the excess term (see Fig. 5). However, the Reynolds term is one order of magnitude smaller than the excess term (see Fig. 5). The viscous term (see Fig. 6) has very small amplitudes for all frequencies of interest and therefore can be neglected. Additionally, it could be shown that the blade passing frequency of $f_{\mathrm{Blade}} = 12000$ Hz most prominently appears in the spectrum of the excess term. Consequently, it seems that the amplitude of the dominant frequency in the spectrum of a $p-t-$signal of a turbocharger compressor, the blade passing frequency $f_{\mathrm{Blade}}$, is dominated by the excess term. Investigating the field FFT of all three

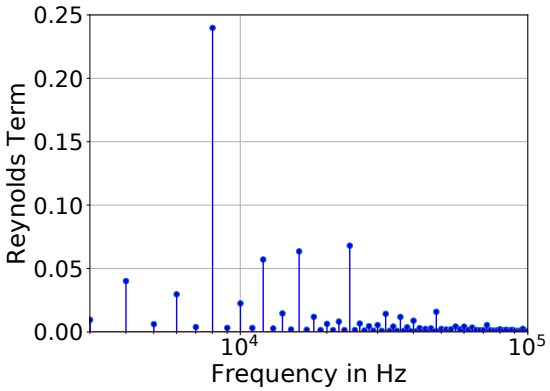


**Figure 4:** Averaged Reynolds term spectra averaged for cells in inlet, impeller, and outlet region, computed with a time step corresponding to 360 steps per turn.

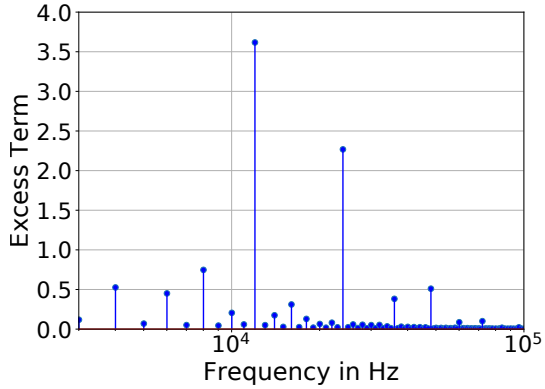


**Figure 5:** Averaged excess term spectra averaged for cells in inlet, impeller, and outlet region, computed with a time step corresponding to 360 steps per turn.

Lighthill source terms showed, that the only source terms with significant amplitudes that are not located inside of the impeller region occur at the blade passing frequency

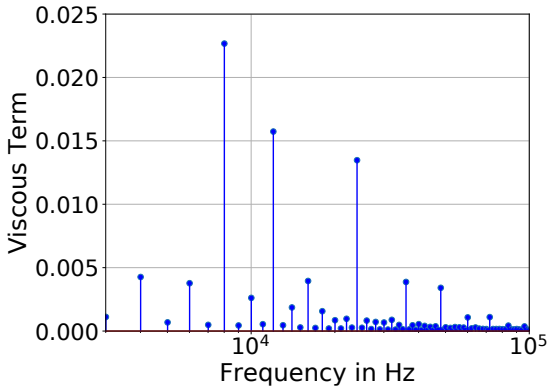


**Figure 6:** Averaged viscous term spectra averaged for cells in inlet, impeller, and outlet region, computed with a time step corresponding to 360 steps per turn.

(BPF) $f_{\mathrm{Blade}}$ or it's harmonics (see Fig. 7). Flow and as a consequence, source terms that are located inside of the rotating impeller region, rotate with the compressor wheel and therefore are not effected by the passing blades. However, the reason that source terms connected to the BPF are mainly located at the outlet, is comprehensible because only the flow in the outlet is upstream the wheel blades and therefore highly effected by the passing blades. Furthermore, it could be shown, that

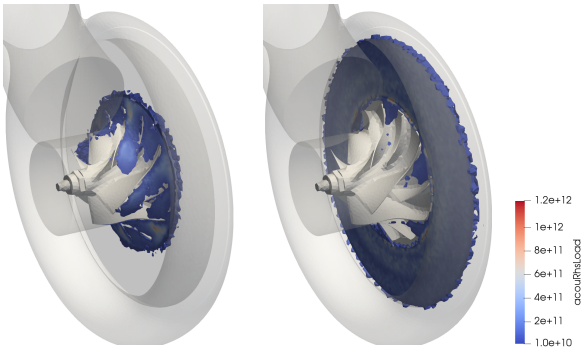


**Figure 7:** Excess source term at $f = 8000$ Hz on the left, and at $f = f_{\mathrm{Blade}} = 12000$ Hz on the right.

only the excess term has significantly large source terms outside of the impeller region. Consequently, noteworthy Reynolds and viscous source terms are mostly concentrating inside of the impeller region, which explains why those source terms don't contribute much at the BPF.

To summarize it can be stated, that the excess term has the most significant source terms. Furthermore, it could be shown that all three source terms that occur at the BPF are mainly located in the outlet region. It should be emphasized that these findings were obtained for an operating point close to the maximum efficiency. Findings for operating points with flow separations cannot be derived from this.

### Different Time Steps

The spectra depicted in Figure 3 shows that two main mechanism for pressure fluctuations occur. The main mechanism, contributing the largest amplitudes, are the

passing blades that generate fluctuations at the BPF $f_{\text{Blade}}$. The second mechanism, can be connected with turbulent structures of the flow inside of the turbocharger compressor. However, fluctuations connected with turbulent phenomenons have much smaller amplitudes than the main mechanism.

Comparing the results of averaged field FFTs of Lighthill's source terms for all three simulations, shows no significant differences. For investigation a relative error is computed, using the simulation with the smallest time step, 3M / 720, as reference. Furthermore, as reference value for scaling the amplitude of $f_{\text{Blade}}$ was used.

$$E^f_{\square} = \frac{|\bar{\square}^f_s - \bar{\square}^f_{\text{3M/720}}|}{\bar{\square}^{f_{\text{Blade}}}_{\text{3M/720}}} \cdot 100\% \,. \tag{6}$$

Turbulent phenomenons are stochastic per definition, and therefore can not be unrestrictedly compared between to different simulations. In the case of frequencies associated with turbulence, a comparison of the source terms leads to large differences with respect to the amplitude of these frequencies. However, because compared to the main mechanism this amplitudes are small, the relevancy of those differences is small. To take this into account, the largest amplitude in the spectrum is used to scale the differences of each frequency to consider the actual relevance of the source terms at that frequency.

Figure 8 shows the relative errors with the amplitude of $f_{\text{Blade}}$ as reference value of the averaged field FFT for the full Lighthill source term. The relative error of all frequencies are small. Computing such a relative error

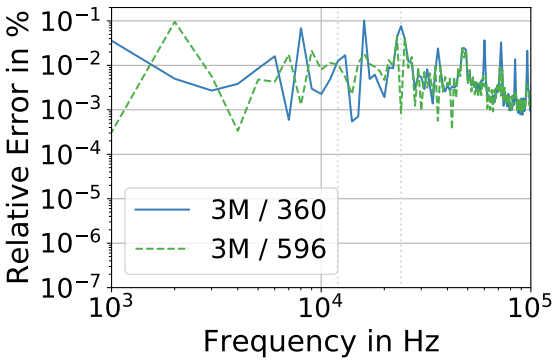


**Figure 8:** Relative error (6) of the averaged field FFT of the full Lightill source term with 3M / 720 as reference. The BPF $f_{\text{Blade}}$ as grey, dotted line.

(6) for the excess term, shows values in the same range as for the full Lighthill source terms. However, the relative error of the averaged field FFT of the Reynolds and viscous terms are about one order of magnitude larger.

This supports the interpretation, that the excess term is mainly influenced by the BPF and density fluctuations connected to the BPF, which is adequately resolved for all three time steps. However, the Reynolds and viscous source term seem to be dominated by turbulent fluctuations, which tend to vary more due to their stochastic nature. This explains their larger relative error.

The computational results presented were obtained using the Vienna Scientific Cluster(VSC)

## Conclusion

It could be shown that for a turbocharger compressor, with an operating point close to the point of highest efficiency, the most dominant source term is the excess term. The Reynolds term is about one order of magnitude smaller, and the viscous term about two orders of magnitude smaller than the excess term. Furthermore, mainly the excess term represents source terms at the blade passing frequency, and those source terms are mostly located in the outlet region. The viscous term can be neglected.

## References

[1] Lighthill, M. J.: On Sound Generated Aerodynamically. I. General Theory, Proceedings of the Royal Society (1952)

[2] Ristorcelli, J. R.: A Closure for the Compressibility of the Source Terms in Lighthill's Acoustic Analogy, ICASE Report (1997)

[3] Kaltenbacher, M.: Computational Acoustics, CISM International Centre for Mechanical Sciences, Volume 579 (2018)

[4] Crighton, D. G., Basic Principles of Aerodynamic Noise Generation, Prog. Aerospace Science (1975)

[5] Howe, M. S., Theory of Vortex Sound (2004)

[6] Arnold G., Zidick C., Charle's law revisited, Journal of Chemical Education (1991)

[7] Broatch A., et al., Simulations and measurements of automotive turbocharger compressor whoosh noise, Engineering Applications of Computational Fluid Mechanics (2015)

[8] Mendonca F., et al., Simulation of Radial Comresspr Aeroacoustics using CFD, Proceedings of ASME Turbo Expo GT (2012)

[9] Broatch A., et al., Methodology for experimental validation of a CFD model for predicting noise generation in centrifugal compressors, International Journal of Heat and Fluid Flow (2014)